Article

The Determination of Dendrite Coherency Point Characteristics Using Three New Methods for Aluminum Alloys

Iban Vicario Gómez [1,*] , Ester Villanueva Viteri [1] , Jessica Montero [2], Mile Djurdjevic [3] and Gerhard Huber [3]

[1] Department of Foundry and Steel Making, Tecnalia Research & Innovation, c/Geldo, Edif. 700, E-48160 Derio, Spain; ester.villanueva@tecnalia.com
[2] Befesa Aluminio, Carretera Lutxana-Asua 13, 48950 Erandio, Spain; jessica.montero@befesa.com
[3] Nemak Linz, Zeppelinstrasse 24, 4030 Linz, Austria; mile.djurdjevic@nemak.com (M.D.); gerhard.huber@nemak.com (G.H.)
[*] Correspondence: iban.vicario@tecnalia.com; Tel.: +34-943-005-511

Featured Application: Increase the accuracy of solidification software for aluminum alloys.

Abstract: The aim of this work is to give an overview of existing methods and to introduce three new methods for the determination of the Dendrite Coherency Point (DCP) for $AlSi_{10}Mg$ alloys, as well as to compare the acquired values of DCP based on a thermal analysis and on the analysis of cooling curves working with only one thermocouple. Additionally, the impact of alloying and contaminant elements on the DCP will be also studied. The first two proposed methods employ the higher order derivatives of the cooling curves. The DCP was determined as the crossing point of the second and third derivative curves plotted versus time (method 1) or that of the temperature (method 2) with the zero line just after the maximum liquidus temperature. The third proposed method is based on the determination of the crossing point of the third solid fraction derivative curve with the zero line, corresponding to a minimum of the second derivative. A Taguchi design for the experiments was developed to study the DCP values in the $AlSi_{10}Mg$ alloy. The DCP temperature values of the test alloys were compared with the DCP temperatures predicted by the previous methods and the influence of the major and minor alloying elements and contaminants over the DCP. The new processes obtained a correlation factor r^2 from 0.954 and 0.979 and a standard deviation from 1.84 to 2.6 °C. The obtained correlation values are higher or similar than those obtained using previous methods with an easier way to define the DCP, allowing for a better automation of the accuracy of DCP determination. The use of derivative curves plotted versus temperature employed in the last two proposed methods, where the test samples did not have an influence over the registration curves, is proposed to have a better accuracy than those of the previously described methods.

Keywords: aluminum alloys; dendrite coherency point; DCP; thermal analysis

1. Introduction

Thin aluminum cast structural parts produced by the Vacuum High Pressure Die Casting (HPDC) process are applied more and more in the automotive industry. Among the many commercial cast aluminum alloys used in HPDC production, the $AlSi_{10}Mg$ alloy has found significant application due to an excellent combination of its high ductility values with a good crush performance of its final cast parts [1].

The solidification of an aluminum alloy begins at the liquidus temperature with the formation of many small crystal nuclei in the molten metal, promoted by melt undercooling. Further cooling leads to a more significant precipitation of the primary dendritic network of α-Al crystals. A dendrite is a tree-like crystal structure that grows in molten metal as the alloy freezes. From a single nucleus, the dendrite grows forward (primary) and laterally (secondary) until the primary dendrite meets another dendrite. The temperature at which this occurs is defined as the dendrite coherency temperature and the solid fraction formed until this temperature is named the dendrite coherency point fraction. The development of the α-aluminum dendritic structure that follows is the growth of the secondary and even tertiary branches with a coarsening of the secondary dendrite arms. Before the molten alloy arrives at the dendrite coherency temperature, the mass feeding of a mixture of the slurry and molten alloy is possible. The impingement of the α-aluminum crystals at the dendrite coherency temperature significantly reduces the flowability of the residual melt and feeding changes from "mass" to inter-dendritic feeding, where the molten metal starts to flow through the solid skeleton of the α-Aluminum dendrites. The solidification of the primary α-aluminum dendrites increases the concentration of the alloying elements in the remaining liquid, promoting the precipitation of AlSi primary eutectic phase, as well other inter-metallics in the hypoeutectic alloys [2]. The major alloying elements have a significant impact on the solidification path of the AlSi alloys, but some minor elements or contaminants can also change the solidification path of those alloys [3]. However, there is a lack of knowledge in the available literature on how different minor alloying elements and contaminants alone or in combination with major alloying elements can impact the DCP temperature in the AlSi$_{10}$Mg alloy, based on the available methods applied to detect this point.

According to many authors [3–11], the DCP marks the point where casting defects such as shrinkage porosity, hot tearing, and macro-segregation start to appear. A good understanding of the solidification phenomena related to DCP and knowledge of the influence of alloying elements and process parameters on this point are needed for the development of new alloys and, especially, for improving the accuracy of simulation procedures, as well as optimizing HPDC processes.

Thermal analysis (TA) is a quite spread quality control system in aluminum casting plants. The solidification path of molten alloys is plotted in a temperature versus time graph. The obtained curve is called the cooling curve and, together with its derivatives, is employed to characterize the solidification path of different alloys. The existing techniques for determination of the DCP are given below.

Based on the extended literature research [1–24], there are four main processes for the determination of DCP temperature:

1. the mechanical (rheological) method,
2. the two thermocouples method using the minimum temperature difference,
3. the single thermocouple method using the minimum of the second derivative of the cooling curve and/or the common point of the second and third derivative in the zero axis,
4. the three thermocouples method determining the thermal diffusivity during solidification.

The mechanical method monitors the torque required to rotate a disc or a paddle in molten aluminum [8,9] until the shear strength value starts to increase its value at the DCP point at a constant rotation speed.

The two thermocouples technique, or the TA method [10,11], determines the temperature in the center (T_C) of a test crucible and at a nearby inner wall (T_W) using two thermocouples. The DCP temperature is determined by the local minimum on the ΔT versus time curve ($\Delta T = T_W - T_C$) and its projection on the T_C cooling curve. Heat removal from the solid phase is faster than from the liquid phase and occurs at the minimum of the ΔT versus time curve because there is a higher thermal conductivity in the solid dendrites than in the surrounding liquid metal.

Other similar methods based on one thermocouple have been developed to decrease costs and increase productivity in the data analysis by reducing the total amount of processed data.

The first method to define the DCP with one thermocouple located in the center of the TA cup is based on the determination of the first minimum point on the plotted second derivative vs. time graph [12–14], as shown in Figure 1.
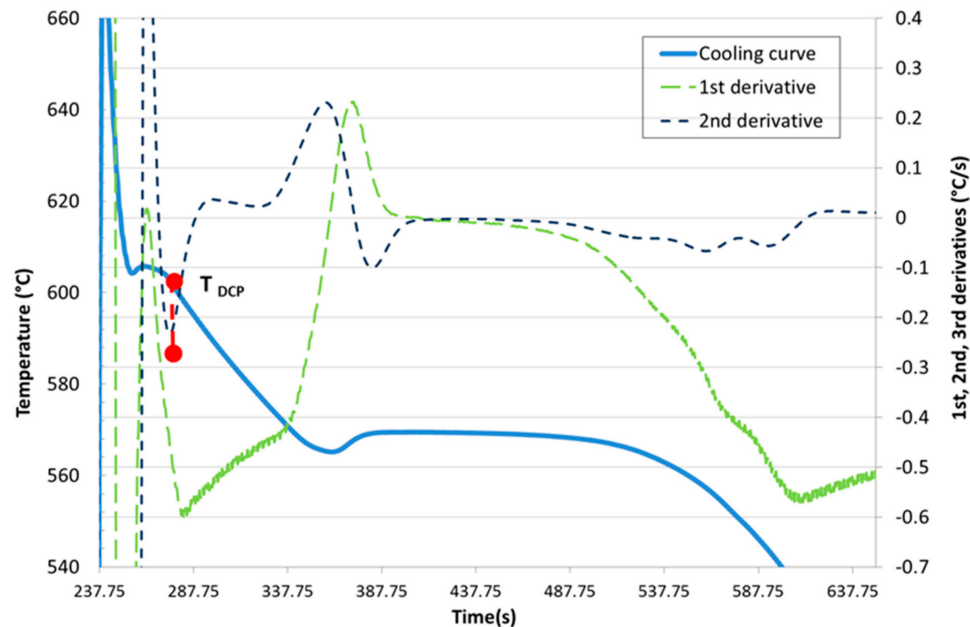

Figure 1. Method 1: the first minimum of the d^2T/dt^2 curve.

The second method with one thermocouple is based on the detection of the first minimum of the first derivative curve plotted vs. time graph [15,16] as shown in Figure 2 with the determination of the maximum liquidus temperature in the first negative crossing of the first derivative curve with the zero line ($T_{liq\,max}$) and the determination of the DCP temperature in the first minimum of the dT/dt curve immediately after the maximum liquidus point.
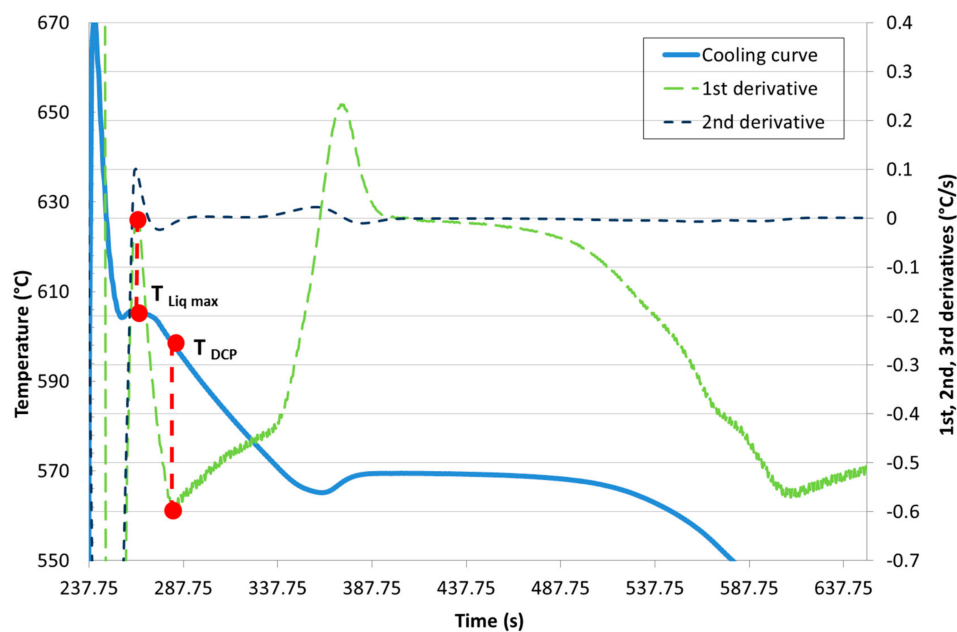

Figure 2. Method 2: the first minimum of the dT/dt curve after $T_{liq\,max}$.

Some works indicate that sometimes the thermal signal is so weak that it is difficult to define the minimum point on the second derivative curve [17].

The third method using only one thermocouple is based on the first derivative curve plotted versus the temperature analysis with the determination of the point at which the first derivative curve starts to change its slope [1], as shown in Figure 3.
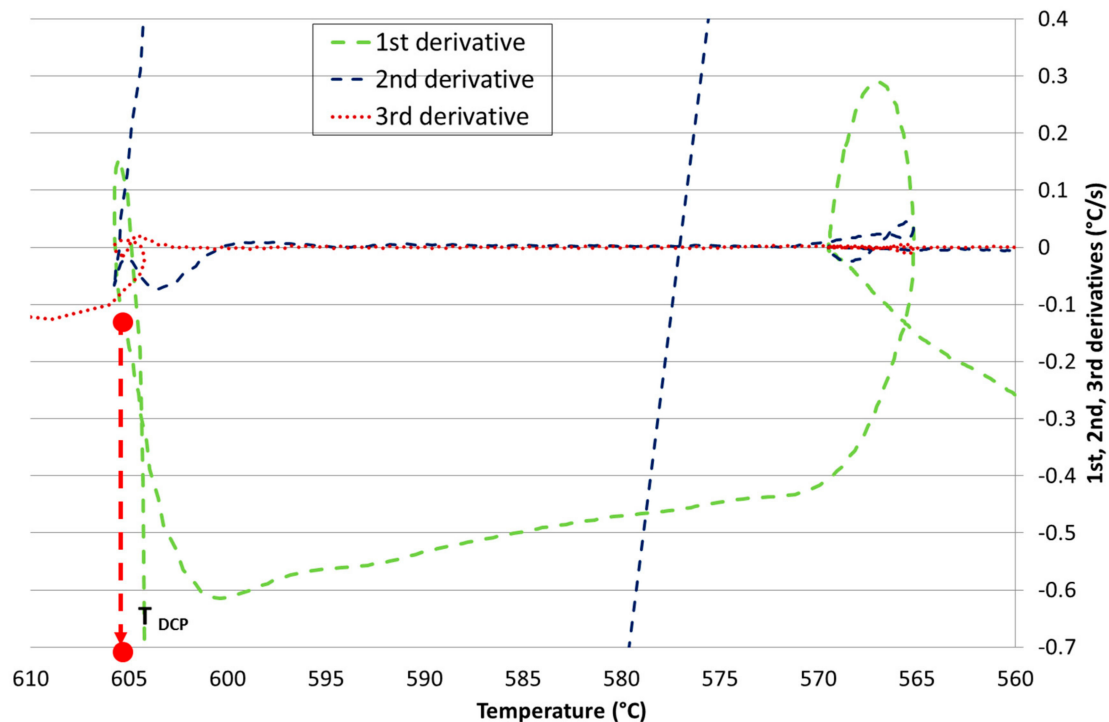

Figure 3. Method 3: dT/dt curve vs. T, with the DCP point in the elbow.

However, it is sometimes difficult to define the exact point of deviation because there are no loops in the first derivative curve, so it is not possible to define the exact position of the elbow point on the dT/dt versus temperature curve.

The solid fraction at the DCP can be determined by using different experimental and/or arithmetic methods [8]. Among them, the Newtonian and Fourier [20–22] methods are mostly applied in the case when the cooling curve data are known.

For the Newtonian analysis, first, the solid fraction at each point or temperature must be calculated, determining the integration or cumulative area between the cooling rate (first derivative (dT/dt) of the cooling curve) and the baseline dT_{BL}/dt (BL). The base line corresponds to a cooling rate curve if there is no phase transformation. Applying this method, it is possible to determine the amount of solid fraction at the dendritic coherence point, identifying the temperature at which this event occurs. This temperature is determined in the elbow of the first derivative of the cooling curve when it starts to be constant. This method is applied as the following Figure 4 exhibits.
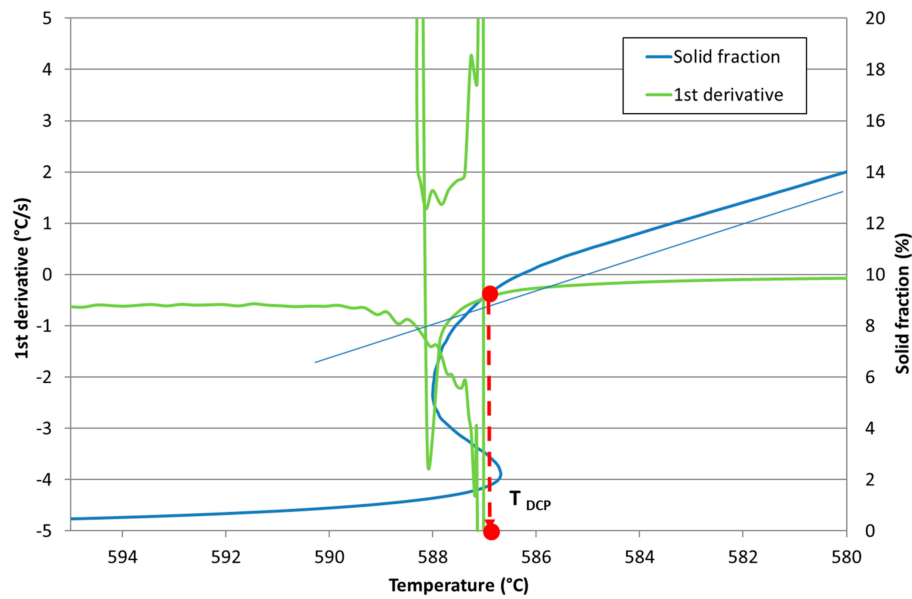
Figure 4. Method 4: dfs/dT curve vs. T, with the DCP point in the elbow.

The determination of the crossing point of the second and third derivative curves plotted versus time after the maximum liquidus point has been proposed as a solution in hypoeutectic ductile iron alloys [23] with only one thermocouple and it is the base for the first proposed method, where the same concept has been employed for hypoeutectic aluminum alloys, as can be observed in Figure 5.
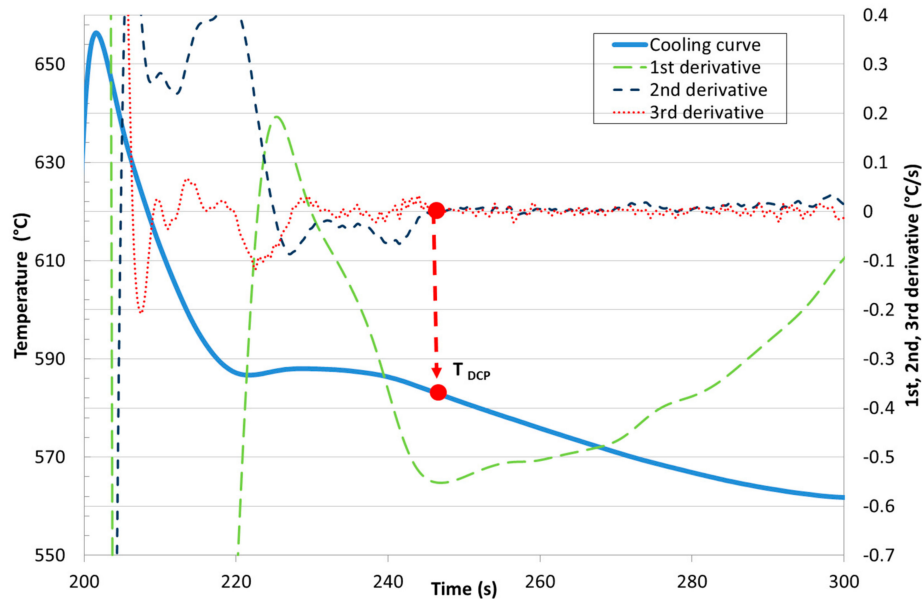
Figure 5. Method 5: the DCP determination at the crossing point of the second and third derivative of dT/dt vs. time.

The three thermocouples method employs thermocouples located at the center of the wall, the middle of the wall, and close to the wall of steel or graphite crucibles, measuring the variation in the thermal diffusivity during the solidification process [24]. We compared this method with the other methods mentioned before concluding that all the previously mentioned methods produced similar results.

This work displays the applicability of all available methods (including the three new methods proposed in this work) for having a pretty accurate trend for the determination of DCP independent on the chemical composition of the investigated alloys. This paper also illustrates that the recording of the solidification temperatures using a single thermocouple can be successfully used to accurately detect the DCP temperature. The proposed methods make the determination of the DCP point easier, especially in the case where there is a lack of information and in the case of the last two proposed methods with no influence of the size of the thermal analysis test samples.

2. Materials and Methods

The approach used in the present work has been based on the identification of the effect of 12 main alloying elements in the solidification parameters through the Taguchi methodology. Two orthogonal matrices were used: an L16 matrix and a modified L8 matrix. The former employs two levels that are related to the maximum and minimum amounts of the alloying element. The modified matrix incorporates intermediate values. To perform a statistical evaluation of results, the Excel software was employed for the determination of the linear regression coefficient (r^2) and the standard deviation (S_{ey}) for the obtained results from the 25 tested alloys. The multiple regression analysis techniques seek to derive a single curve that represents the general trend of the data to make extrapolations beyond the limits of the observed data or interpolations. As much of the equations were obtained with a very limited amount of data (25 alloy compositions), they should be used as trend indicators. It is recommended that at least 100 observations (different alloys) be used to ensure a high degree of accuracy.

The base alloy for the developments has been chosen from the most commonly used alloys for HPDC, and alloying elements were added to the melt to obtain the desired compositions. No grain refining or silicon modification master alloys were added to the melts. The selected alloy is $AlSi_{10}Mg$ according to the standard EN AC-43.400 included in the EN 1706:2010 standard. To determinate the obtained alloy composition, a SPECTROMAXx arc spark OES metal analyzer was used. The obtained compositions are given in Table 1.

Table 1. The compositions of base alloys (mass %).

Ref.	Si	Mg	Fe	Cu	Ni	Cr	Mn	Ti	Zn	Pb	Sn	Sr
[1]	9.00	0.30	0.38	0.03	0.00	0.01	0.34	0.02	0.01	0.00	0.002	0.021
[2]	8.02	0.19	0.29	0.02	0.00	0.01	0.21	0.01	0.00	0.00	0.003	0.003
[3]	8.66	0.14	0.30	0.02	0.00	0.01	0.21	0.20	0.29	0.27	0.039	0.014
[4]	10.01	0.69	0.34	0.02	0.23	0.15	0.67	0.02	0.01	0.00	0.002	0.06
[5]	9.75	0.68	0.34	0.023	0.226	0.145	0.72	0.121	0.347	0.138	0.064	0.055
[6]	8.77	0.15	0.85	0.19	0.21	0.16	0.21	0.12	0.16	0.21	0.073	0.006
[7]	8.43	0.11	0.91	0.19	0.19	0.14	0.18	0.19	0.18	0.19	0.066	0.047
[8]	9.02	0.38	1.05	0.29	0.21	0.07	0.81	0.17	0.06	0.21	0.019	0.048
[9]	9.26	0.56	0.73	0.09	0.001	0.069	0.53	0.024	0.212	0.01	0.002	0.007
[10]	11.65	0.58	0.34	0.199	0.196	0.017	0.302	0.239	0.028	0.073	0.032	0.021
[11]	10.54	0.52	0.34	0.16	0.15	0.02	0.31	0.17	0.23	0.26	0.026	0.053
[12]	11.49	0.40	0.91	0.42	0.00	0.14	0.67	0.23	0.15	0.18	0.04	0.046
[13]	11.60	0.46	0.83	0.18	0.00	0.18	0.74	0.02	0.19	0.23	0.003	0.007
[14]	11.64	0.53	0.96	0.08	0.08	0.16	0.08	0.27	0.13	0.08	0.033	0.01
[15]	11.82	0.52	0.96	0.11	0.11	0.14	0.11	0.11	0.18	0.11	0.046	0.023
[16]	11.41	0.35	0.95	0.27	0.30	0.09	0.69	0.25	0.09	0.25	0.026	0.038
[17]	12.07	0.28	0.83	0.13	0.17	0.03	0.49	0.08	0.02	0.16	0.055	0.033
[18]	10.21	0.278	0.43	0.052	0.001	0.069	0.333	0.021	0.083	0.001	0.002	0.013
[19]	10.37	0.28	0.50	0.11	0.00	0.14	0.44	0.02	0.01	0.00	0.002	0.009
[20]	10.64	0.63	0.41	0.05	0.00	0.07	0.33	0.02	0.10	0.00	0.001	0.013

Table 1. *Cont.*

Ref.	Si	Mg	Fe	Cu	Ni	Cr	Mn	Ti	Zn	Pb	Sn	Sr
[21]	10.31	0.29	0.54	0.09	0.00	0.11	0.35	0.01	0.01	0.00	0.002	0.006
[22]	10.80	0.52	0.48	0.052	0.001	0.064	0.334	0.028	0.095	0.002	0.002	0.014
[23]	10.90	0.43	0.51	0.10	0.00	0.11	0.47	0.01	0.02	0.00	0.005	0.006
[24]	11.71	0.442	0.57	0.073	0.002	0.075	0.438	0.016	0.042	0.002	0.002	0.013
[25]	10.73	0.355	0.6	0.099	0.001	0.087	0.384	0.016	0.102	0.001	0.002	0.009

The procedure to acquire the cooling curve is very simple. Liquid aluminum melt is preheated to approximately 100 °C (720 °C in our case) above its liquidus temperature. To obtain cooling curves by Thermal Analysis (TA), the samples with masses of approximately 300 ± 10 g were poured into calibrate sand cups with a T-type thermocouple placed in the middle of the cup. Temperatures between 630–400 °C were recorded. The data of the TA were collected using a high-speed National Instruments Data Acquisition System linked to a personal computer. Each TA trial was repeated three times. The obtained cooling rate was approximately 3 °C/s.

Development of New Methodologies for the Determination of DCP Temperature

The first proposed method is based on previous work developed for the detection of DCP in hypoeutectic iron alloys [23]. The temperature of the DCP is determined as the crossing point of the second and third derivative curves plotted versus time, with the zero line placed nearly after the maximum liquidus temperature. This point reflects the point where the cooling rate becomes constant.

We can observe the determination of the DCP point for the first proposed method in Figure 6.
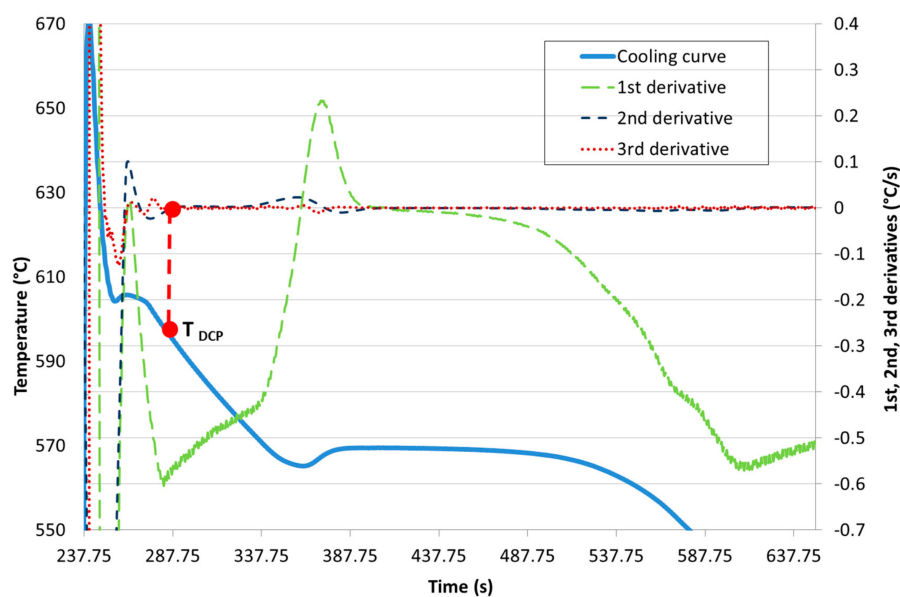

Figure 6. Method 5: the DCP determination in the crossing point of the second and third derivative in the zero axis of the dT/dt curve.

We can observe that the crossing point is closed to the minimum of the first derivative.

The second method is based on the determination of the crossing point of the second and third derivative curves plotted versus temperature with a zero line that corresponds to the DCP. This DCP also reflects the point after which the cooling rate becomes constant. Therefore, in this method, the detection of this point is easier and more accurate compared to the previous methods in which the DCP point was determined at the elbow point of the first derivative curve (dT/dt) with less accuracy. In Figure 7, the determination of the DCP point for the third proposed method is represented.
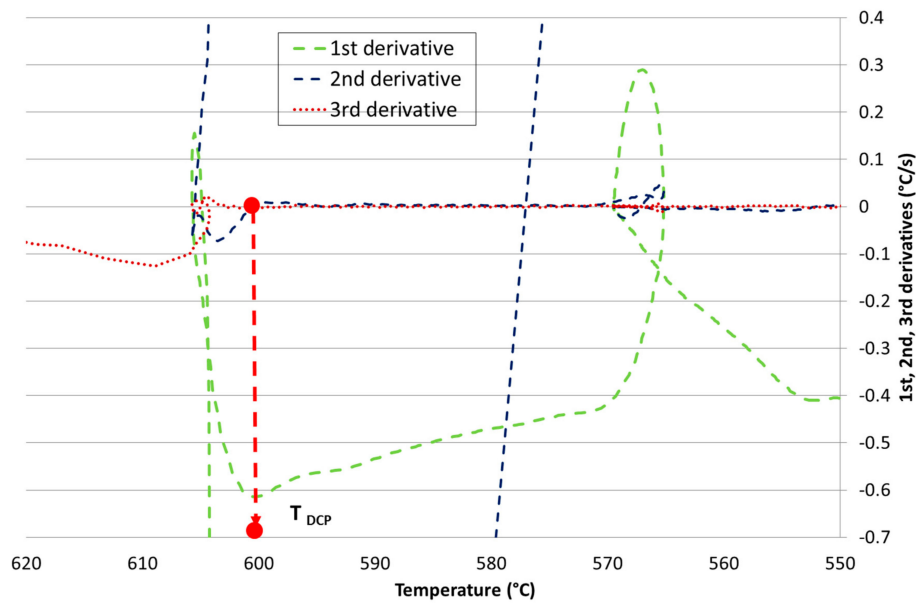
Figure 7. Method 6: the DCP determination at the crossing point of the second and third derivative of dT/dt vs. T curve.

We can observe that the crossing point is close to the minimum of the first derivative.

The third proposed method is based on the determination of the crossing point of the third derivative curve with the zero line of the solid fraction (dFs/dt) plotted versus temperature. This point also corresponds to a minimum in the second derivative. The DCP Temperatures can be determined easily because the size of the thermal analysis test samples does not have as much of an influence over the registration curves as the temperature, which is a thermodynamically extensive property.

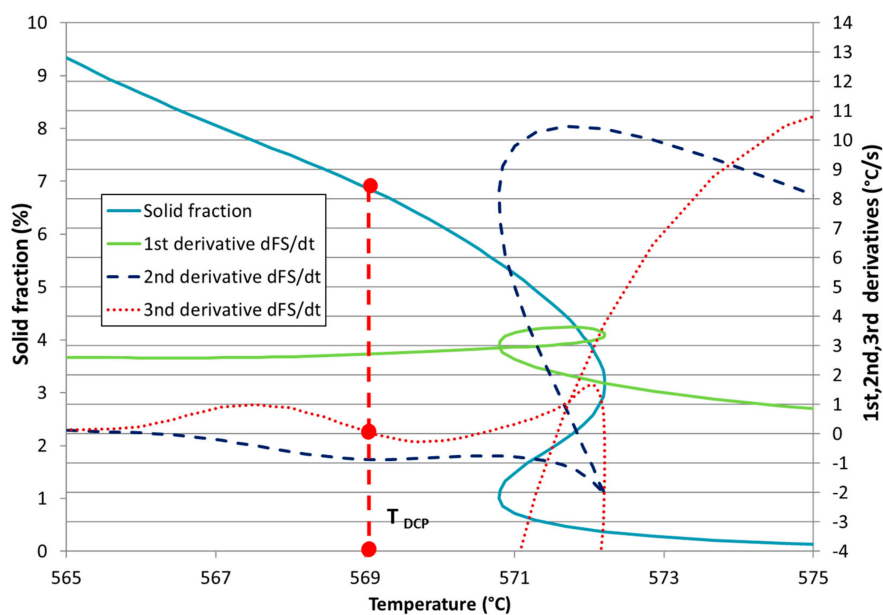We can observe the determination of the DCP point for the second proposed method in Figure 8.

Figure 8. Method 7: the DCP determination at the crossing point of the third derivative of dfs/dt vs. T curve with the zero line.

3. Results

The dendrite coherency temperatures of the studied alloys were determined by applying various methods based on the analysis of the cooling curves and their corresponding derivatives using one thermocouple placed at the center of the test cup. Table 2 summarizes all these temperatures.

Table 2. The DCP temperature values of the studied alloys DCP (°C).

Ref.	Method 1	Method 2	Method 3	Method 4	Method 5	Method 6	Method 7
[1]	590.8	591.6	590.54	591.7	586.82	587.6	590.29
[2]	603.8	599.12	604.46	605.7	599.12	600.47	603.2
[3]	599.82	590.98	599.98	600.0	590.975	590.8	593.31
[4]	585.94	582.47	586.60	587.9	583.03	582.875	585.93
[5]	582.14	575.61	583.19	583.2	575.605	574.945	580.32
[6]	590.25	587.38	594.89	594.9	587.375	587.37	590.2
[7]	598.39	589.62	597.68	598.3	589.615	589.865	593.57
[8]	590.55	586.74	593.53	593.5	586.74	586.72	590.33
[9]	590.8	589.92	592.19	592.1	589.92	588.03	590.56
[10]	576.01	570.32	576.46	576.5	570.32	570.865	575.01
[11]	582.04	573.85	583.05	583.1	573.85	574.46	578.385
[12]	576.17	571.68	576.50	576.5	571.68	571.97	570.425
[13]	572.58	570.01	572.89	573.2	570.005	569.46	572.44
[14]	574.91	568.47	575.32	575.3	568.47	569.085	574.465
[15]	569.96	567.4	570.84	572.0	567.395	567.615	569.405
[16]	575.94	571.3	576.59	576.6	571.3	571.54	571.585
[17]	569.09	567.29	568.79	570.4	567.29	567.82	569.455
[18]	582.8	577.69	583.16	583.8	577.69	578.05	581.815
[19]	583.92	575.97	584.49	585.2	575.965	576.27	583.675
[20]	578.54	575.14	578.23	579.4	575.14	575.77	578.4
[21]	585.08	581.73	586.08	587.2	581.725	582.465	584.585
[22]	577.77	573.61	578.67	579.1	573.61	573.78	576.92
[23]	579.22	576.42	580.98	581.4	576.415	576.7	578.795
[24]	573.8	570.7	575.04	575.2	570.695	570.975	573.2
[25]	579.75	576.17	580.93	581.1	576.17	576.36	579.27

To compare the temperature values obtained for every method and their tendencies, a comparison graph is represented in Figure 9.
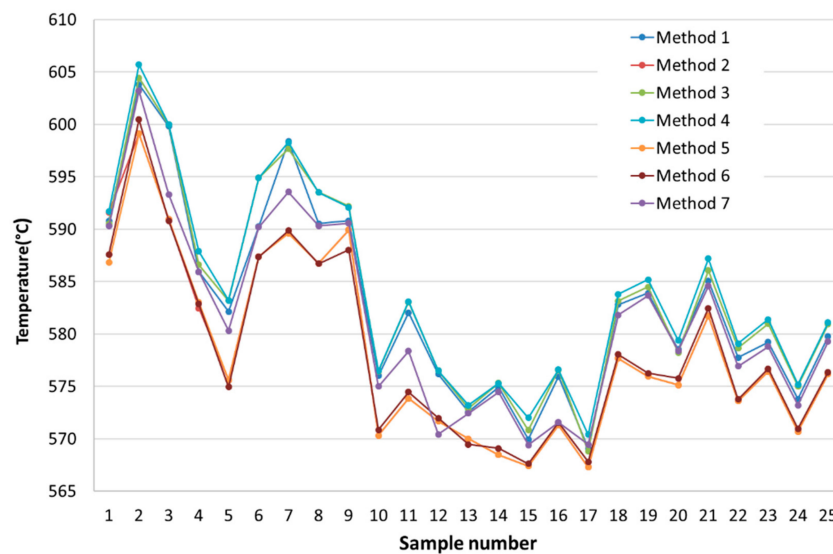

Figure 9. The comparison of the DCP temperatures for every sample with the studied methods.

As it can be observed from Figure 9, all the obtained DCP temperatures could be divided into three groups. The applied methods (methods 2, 5 and 6) detected similar values for DCP. All these values have slightly lower DCP temperatures than those obtained using the other methods. The DCP temperatures detected using methods 1, 3 and 4 are characterized by slightly higher DCP temperatures. The DCP temperatures determined using method 7 are mostly located in the middle, between the two recognized temperature areas. However, it can be observed that all the applied methods are very sensitive to changes in the chemical composition of the investigated alloys.

By using linear regressions calculations with the obtained values of DCP temperatures, Equations (1) to (7) can be written. Some statistical parameters such as the linear regression coefficient (r^2) and the standard deviation (S_{ey}) can also be observed. To define the influence of every alloying element on the studied properties, statistical student t (t) values are employed. The *t*-test is a statistical hypothesis test in which the test statistic follows a Student's t-distribution under the null hypothesis. In our case, the values > 2.66 represent that the selected alloying element has a significant influence over the studied parameters and the "0" values represent that the studied alloying element does not have any influence over the studied parameters (null hypothesis). An intermediate "t" value between 0 and 2.66 shows that the studied parameter has an influence over the DCP temperature, with a higher influence the closer the value is to 2.66, despite not having a statistical influence.

Method 1

$$T_{DCP} (^{\circ}C) = 661.37 - 7.18Si - 6.07Mg - 3.20Fe - 3.33Cu - 6.94Ni + 6.12Cr\text{-}0.59Mn + 23.59Ti - 5.70Zn + 1.69Pb - 53.79Sn + 14.72Sr; r^2 = 0.977; S_{ey} = 1.99.$$ (1)

Method 2

$$T_{DCP} (^{\circ}C) = 657.2 - 7.60Si + 3.54Mg + 3.14Fe - 3.59Cu\text{-}10.78Ni - 14.20Cr + 2.08Mn + 3.97Ti - 17.71Zn + 5.26Pb + 1.21Sn - 27.38Sr; r^2 = 0.976; S_{ey} = 2.39.$$ (2)

Method 3

$$T_{DCP} (^{\circ}C) = 665.71 - 7.65Si - 3.16Mg - 3.21Fe + 3.24Cu - 0.62Ni + 7.1Cr - 0.69Mn + 17.84Ti - 5.99Zn + 3.4Pb - 45.53Sn - 32.19Sr; r^2 = 0.977; S_{ey} = 2.02.$$ (3)

Method 4

$$T_{DCP} (^{\circ}C) = 666.92 - 7.67Si - 2.26Mg - 3.01Fe + 1.76Cu - 3.15Ni + 7.00Cr - 1.77Mn + 13.23Ti - 11.42Zn + 6.33Pb - 34.09Sn - 14.18Sr; r^2 = 0.977; S_{ey} = 2.05.$$ (4)

Method 5

$$T_{DCP} (^{\circ}C) = 654.69 - 7.38Si + 2.3Mg + 2.30Fe - 0.89Cu - 5.96Ni - 6.15Cr - 9.16Mn + 3.55Ti - 13.41Zn + 3.96Pb - 9.34Sn - 39.17Sr; r^2 = 0.\ 954; S_{ey} = 2.60.$$ (5)

Method 6

$$T_{DCP} (^{\circ}C) = 655.47 - 7.31Si + 2.43Mg + 1.47Fe - 0.86Cu - 7.87Ni - 8.04Cr + 0.16Mn + 4.20Ti - 19.26Zn + 6.69Pb - 7.06Sn - 26.46Sr; r^2 = 0.960; S_{ey} = 2.46.$$ (6)
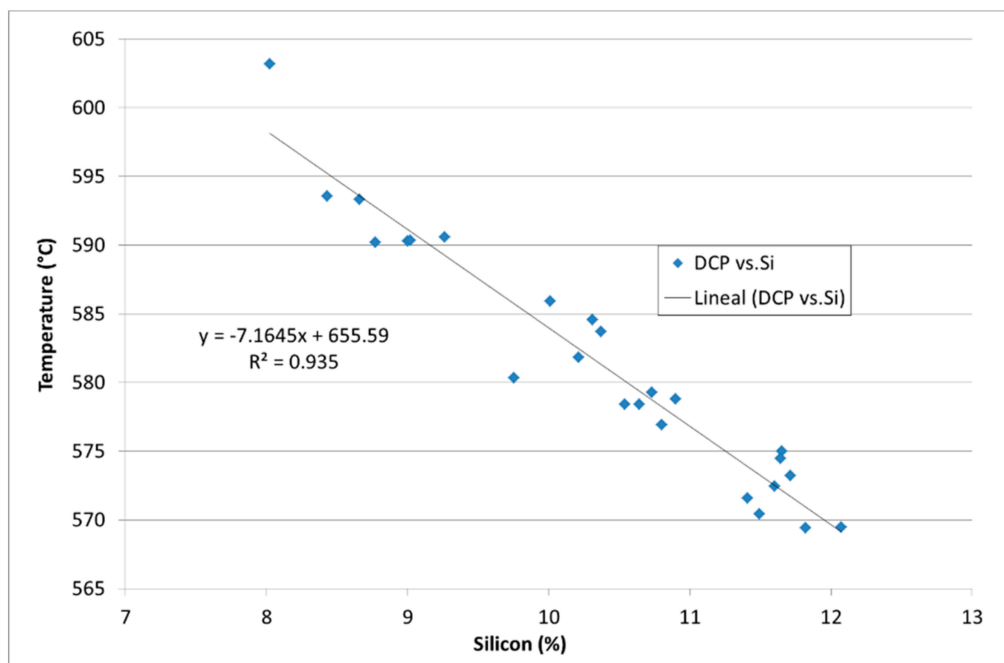
Method 7

$$T_{DCP} (^{\circ}C) = 661.64 - 7.55Si + 2.70Mg - 0.25Fe - 7.39Cu - 3.21Ni + 3.46Cr - 0.34Mn + 9.79Ti - 18.85Zn + 5.41Pb - 20.40Sn - 40.57Sr; r^2 = 0.979; S_{ey} = 1.84.$$ (7)

The student "t" coefficients for temperature DCP obtained by each one of the regressions are shown in the following Table 3.

Table 3. The student "t" coefficients for T_{DCP}.

Meth.	Si	Mg	Fe	Cu	Ni	Cr	Mn	Ti	Zn	Pb	Sn	Sr
1	**13.57**	1.17	1.22	0.39	0.79	0.6	0.18	2.65	0.56	0.16	1.42	0.4
2	**11.95**	0.57	0.99	0.35	1.02	1.17	0.51	0.37	1.45	0.42	0.03	0.61
3	**14.23**	0.6	1.2	0.37	0.07	0.69	0.2	1.97	0.58	0.32	1.18	0.85
4	**14.09**	0.42	1.11	0.2	0.35	0.67	0.51	1.44	1.09	0.6	0.87	0.37
5	**10.65**	0.4	0.67	0.08	0.52	0.69	0.4	0.3	1.01	0.29	0.19	0.8
6	**11.16**	0.38	0.45	0.08	0.72	0.64	0.04	0.38	1.54	0.52	0.15	0.57
7	**15.45**	0.56	0.1	0.94	0.39	0.37	0.11	1.19	2.01	0.57	0.58	1.18

If we obtain a representation of the statistical effect of silicon over the DCP temperature, we can observe that its linear regression coefficient is 0.935, for example, if we employ the calculations of method 7, as shown in Figure 10, it is not as good as the obtained 0.979 value, including the rest of alloy elements.

Figure 10. The effect of the Si percentage over the dendrite coherency point temperature with method 7.

4. Discussion

The proposed methods overcame the problems detected to make an accurate determination of the DCP temperature. The determination of the DCP point is very simple and done with a good accuracy in comparison to previous methods, with only one thermocouple, promoting an increased productivity with a low cost in the data analysis.

There is a similar tendency in the DCP values in all the methods in relation to the variation of the alloy composition. Methods 1, 3, and 4 show a tendency to have higher DCP temperatures values because the acceleration of the cooling rate is the basis of defining the exact point at which the DCP starts in these methods, where a limited number of dendrites touch one to another, but promote the increase of the cooling rate in the sample. The rest of the methods are based on the determination of the exact moment when the cooling speed is constant, so all the dendrites touch one to another.

From the studied methods, we estimate that method 6 and method 7 could be the ones with the better trend accuracy due to the fact that the use of the derivative curves plotted versus temperature is not as influenced by the size of the thermal analysis test samples on the registration curves as the

temperature, which is a thermodynamically extensive property. Additionally, very similar values were obtained from both methods. In the case of method 3, where the dT/dt curve is plotted vs. T with the DCP point in the elbow, and method 4, in which the dfs/dT curve vs. T exists with the DCP point in the elbow, there is no clear indication of which one is the exact point and it is also very complicated to obtain a curve showing a perfect elbow.

The only element that has a direct effect in the studied alloys with a significant statistical influence over the TDCP is Si, with a lower impact than the other alloying elements. The increase in the percentage of Si promotes a decrease in TDCP. This is an expected behavior because it is well known that an increase in the Si% decreases the solidification interval of hypoeutectic aluminum alloys and their related characteristic solidification temperatures until the minimum solidification temperature interval is reached by eutectic composition [24]. The obtained formulae should be taken as trend indicators [25] and, taking this into account, Ni and Zn show a tendency to decrease the TDCP. It is known that an increase in the Zn% decreases the characteristic solidification temperatures of hypoeutectic aluminum alloys because the Zn enters into the solid dissolution in the alloy matrix and not into the grain boundary, avoiding the enrichment of Zn into the remaining inter-dendritic liquid metal. The decrease of the TDCP is not as expected in the case of Ni and it could be related to the formation of Al_3Ni intermetallic compounds that are precipitated in the beginning of the solidification process of the alloy, at temperatures well above the TDCP and as described in Reference [26] because Ni provides significant changes in the sequence of post-eutectic reactions, promoting a substantial reduction in the alloy's freezing range. In both cases, the obtained results confirm the results obtained for the development of the Si equivalent method for obtaining the solidification temperatures, where Ni and Zn have a positive value, which means that they have an influence on decreasing the solidification temperatures [27,28].

Ti is usually employed in the aluminum industry because it promotes the grain refinement of the aluminum alloys. If the grain is smaller, there are more dendrites in the solidification process, so their tips could touch one to another quicker, increasing the T_{DCP} value, but without statistical relevance. The obtained results could also be correlated with the previous studies so that they show that an alloy refined with Ti has higher solidification temperatures than the unrefined alloys [15,22]. Pb is usually precipitated in the grain boundary as isolated points and has a very restricted solid dissolution in the aluminum matrix. Because of this, Pb could tend to increase the T_{DCP} value, but also without a statistical relevance. This result is also in concordance with a previous study [27,29], where elements such as grain refiners (Ti and B) and silicon modifiers (Sr and Sb) or elements with a low melting point (Bi and Pb) have similar effects on the Si Equivalent value.

The rest of the alloying elements also have a slight influence on the solidification temperature interval, but it is not very important and there is a complex interaction between them, obtaining a better adjustment of the results by adding all the alloying elements. The difference in the increase or decrease of the rest of the alloying elements can be related to the presence of intermetallic or eutectic compounds. If they precipitate before the DCP, they would decrease the T_{DCP}. Many of the alloying element could precipitate in different inter-metallics and eutectics (For example the Fe as Al_5FeSi, $Al_8FeMg_3Si_6$, and others).

By comparing the studied methods, the linear regression coefficient (r^2) and the standard deviation (S_{ey}) show that in all the cases, a good correlation between the developed formulae and the obtained results in r^2 values > 0.95 and Sey from 1.84 to 2.6 °C.

More investigations with torque measurements should be done in order to define which one of the proposed methods is more exact in real DCP point determination and in the correlation between the different quantities of inter-metallics, types, and concentrations to have an estimation of the influence of the different inter-metallics over the T_{DCP}.

5. Conclusions

A Taguchi based methodology has been employed to calculate the DCP and its temperature. The obtained results presented in this paper show the importance of the composition of the alloy over the DCP temperatures and the differences over the different calculation methods. The results show that the obtained equations allow us to define, with good accuracy, the DCP point of any alloy of the $AlSi_{10}Mg$ family, with a good statistical correlation between the obtained values from the different methods, especially with the newly developed methods.

Silicon is the element with the main influence over the DCP point value, but the rest of the alloying elements, despite not having a statistical signification, have an influence over the final DCP temperature.

The determination of the DCP point employing the point where the second and the third derivative crosses after the maximum liquidus temperature point allows us to obtain, in an easier way, the exact DCP point. Additionally, in the case of employing the determination with the dfs/dt vs. T curve, from the developed new methods, the two based on plotting derivatives versus temperature are supposed to obtain the DCP with a higher accuracy than those obtained by previous methods. These techniques allow for a better automatization of the DCP point determination to be used with TA equipment and simulation software with a reduced cost using only one thermos-couple.

Further studies could correlate the obtained values with the Thermocalc software calculated values, not only for the DCP but also for the Solidification fraction with more alloy test to increase the accuracy of the results will be developed. Additionally, the improvement of solidification simulation software and the calculation of DCP with different alloy compositions will be developed by the mechanical (rheological) method and by the two thermos-couple methods.

References

1. Voncina, M.; Mrvar, P.; Medved, J. Thermodynamic analysis of $AlSi_{10}Mg$ alloy. *RMZ M&G* **2006**, *52*, 621–633.
2. Djurdjevic, M.B.; Huber, G. Determination of rigidity point/temperature using thermal analysis method and mechanical technique. *J. Alloys Compd.* **2014**, *590*, 500–506. [CrossRef]
3. Djurdjevic, M.B.; Stockwell, T.; Sokolowski, J. The effect of Strontium on the microstructure of the Aluminium-silicon and Aluminium-copper eutectics in the 319 Aluminium alloy. *Int. J. Cast Met. Res.* **1999**, *12*, 67–73. [CrossRef]
4. Arnberg, L.; Chai, G.; Bäckerud, L. Determination of dendritic coherency in solidification melts by rheological measurements. *Mater. Sci. Eng. A* **1993**, *173*, 101–103. [CrossRef]
5. Chai, G.; Backerud, L.; Avnberg, L. Study of dendrite coherency in Al-Si alloys during equiaxed dendritic solidification. *Z. Metalk.* **1995**, *86*, 54–59.
6. Chai, G.; Bäckerud, L.; Rolland, T.; Arnberg, L. Dendrite coherency during equiaxed solidification in binary aluminum alloys. *Met. Mater. Trans. A* **1995**, *26*, 965–970. [CrossRef]
7. Veldman, N.; Dahle, A.; St. John, D. Determination of dendrite coherency point. In Proceedings of the Die Casting & Tooling Technology Conference, Melbourne, Australia, 22–25 June 1997; pp. 22–25.
8. Bäckerud, L.; Chai, G.; Tamminen, J. *Solidification Characteristics of Aluminum Alloys. Vol. 2. Foundry Alloys*; American Foundrymen's Society. Inc.: Oslo, Norway, 1990; p. 266.
9. Claxton, R. Aluminum alloy coherency. *J. Miner. Met. Mater. Soc.* **1975**, *27*, 14–16. [CrossRef]

10.   Bäckerud, L.; Chalmers, B. Some aspects of dendritic growth in binary alloys: study of the Aluminum–Copper system. *Trans. Met. Soc. AIME* **1969**, *245*, 309–318.

11.   Tamminen, J. Thermal Analysis for Investigation of Solidification Mechanisms in Metals and Alloys. Ph.D. Thesis, Stockholm University, Stockholm, Sweden, January 1988.

12.   Jiang, H.; Kierkus, W.T.; Sokolowski, J.H. Dendrite coherency point determination using thermal analysis and rheological measurements. In Proceedings of the International Conference on Thermophysical Properties of Materials (TPPM), Singapore, 17–19 November 1999.

13.   Djurdjevic, M.B.; Kierkus, W.T.; Sokolowski, J.H. Detection of the dendrite coherency point of Al 3XX series of alloys using a single sensor thermal analysis technique. In Proceedings of the 40th Annual Conference of Metallurgists of CIM, Toronto, ON, Canada; 2001.

14.   Djurdjevic, M.B.; Kierkus, W.T.; Liliac, R.E.; Sokolowski, J.H. Extended analysis of cooling curves. In Proceedings of the 41st Annual Conference of Metallurgists of CIM, Montreal, QC, Canada, 11–14 August 2002.

15.   Pelayo, G.; Sokolowski, J.H.; Lashkari, R.A. Case based reasoning aluminium thermal analysis platform for the prediction of W319 Al cast component characteristics. *J. Achiev. Mater. Manuf. Eng.* **2009**, *36*, 7–17.

16.   Pavlovic-Krstic, J. Impact of Casting Parameters and Chemical Composition on the Solidification Behaviour of Al-Si-Cu Hypoeutectic Alloy. Ph.D. Thesis, Universität Magdeburg, Magdeburg, Germany, 2010.

17.   Djurdjevic, M.B.; Sokolowski, J.H.; Odanovic, Z. Determination of dendrite coherency point characteristics using first dericative curve versus temperature. *J. Therm. Anal. Calorim.* **2012**, *109*, 875–882. [CrossRef]

18.   Jiang, H.; Kierkus, W.T.; Sokolowski, J.H. Determining dendrite coherency point characteristics of Al alloys using single-thermocouple technique. *Trans. Am. Foundrymen's Soc.* **1999**, *68*, 169–172.

19.   Djurdjevic, M.B.; Vicario, I. Description of hypoeutectic Al-Si-Cu Alloys based on their known chemical compositions. *Rev. Metal.* **2013**, *49*, 161–171.

20.   Hosseini, V.A.; Shabestari, S.G. Study on the eutectic and post-eutectic reactions in LM13 aluminum alloy using cooling curve thermal analysis technique. *J. Therm. Anal. Calorim.* **2016**, *124*, 611–617. [CrossRef]

21.   Marchwica, P.; Sokolowski, J.H.; Kierkus, W.T. Fraction solid evolution characteristics of AlSiCu alloys—Dynamic Baseline Approach. *J. Achiev. Mater. Manuf. Eng.* **2011**, *47*, 115–136.

22.   Anjosa, V.; Deike, R.; Silva Ribeiro, C. The use of thermal analysis to predict the dendritic coherency point on nodular cast iron melts. *Ciênc. Tecnol. Mater.* **2017**, *29*, 27–33. [CrossRef]

23.   Zamarripa, R.C.; Ramos-Salas, J.A.; Talamantes-Silva, J.; Valtierra, S.; Colas, R. Determination of the dendrite coherency point during solidification by means of thermal diffusivity analysis. *Met. Mater. Trans. A* **2007**, *38*, 1875–1879. [CrossRef]

24.   Rana, R.S; Purohit, S.; Das, S. Reviews on the influences of alloying elements on the microstructure and mechanical properties of aluminum alloy composites. *IJSRP* **2012**, *2*, 1–7.

25.   Makhlouf, M.; Apelian, D.; Wang, L. Microstructures and Properties of Aluminum die Casting Alloys. 1998. Available online: http://www.osti.gov/biblio/751030 (accessed on 23 July 2018).

26.   Rakhmonov, J.; Timelli, G.; Bonollo, F. Characterization of the solidification path and microstructure of secondary Al-7Si-3Cu-0.3Mg alloy with Zr, V and Ni additions. *Mater. Charact.* **2017**, *128*, 100–108. [CrossRef]

27.   Hernandez, F.C.R.; Djurdjevic, M.B.; Kierkus, W.T.; Sokolowski, J.H. Calculation of the liquidus temperature for hypo and hypereutectic aluminum silicon alloys. *Mater. Sci. Eng. A* **2005**, *396*, 271–276. [CrossRef]

28.   Djurdjevic, M.B.; Francis, R.; Sokolowski, J.H.; Emadi, D.; Sahoo, M. Comparison of different analytical methods for the calculation of latent heat of solidification of 3XX aluminum alloys. *Mater. Sci. Eng. A* **2004**, *386*, 277–283. [CrossRef]

29.   Djurdjevic, M.B.; Tekfak, J.; Odanovic, Z. Applications de l'analysis thermique dans les fonderies d'aluminium. *Fonderie* **2012**, *26*, 31–37.